ELSEVIER

Earth and Planetary Science Letters 179 (2000) 379–390

EPSL

www.elsevier.com/locate/epsl

Non-random spectral components in the seismicity of NE Italy

Carla Braitenberg *

Department of Earth Sciences, University of Trieste, via Weiss 1, 34100 Trieste, Italy

Received 1 December 1999; accepted 12 April 2000

Abstract

The time evolution of seismicity in one of the most active seismic areas of the Alpine Arc has been investigated with the aim of detecting statistically reliable non-random features. The statistical evaluation regards the spectral analysis of the fluctuations of earthquake occurrence with respect to the mean seismicity. The seismic catalogue of the seismometric network of Friuli–Venezia Giulia (NE Italy) (Istituto Nazionale Oceanografia e Geofisica Sperimentale, OGS) is used, limiting the magnitudes to $M \geq 1.8$ and covering the time period from 1977 to 1997. The analysis is carried out on the full and on the aftershock-depleted catalogue. The result is that a significant spectral peak is found, centered on the period of 1.4 years. At the present stage, some doubt remains whether the fluctuations really reflect variations in natural seismicity, or whether they are connected to varying levels of completeness in the data acquisition. A spectral peak of about 1.4 years is also found in the variations of the water table, calculated over the same time interval.

Keywords: induced earthquakes; spectral analysis; water table

1. Introduction

The search for non-random features in natural seismicity has been made in the past with different aims. Either the possible effect of a triggering mechanism was looked for, as for example the earth tides (e.g. [1]), or the space–time–magnitude interrelation was studied with the aim of finding some relations which could be applied in hazard estimates (e.g. [2]). As has been pointed out by Kagan and Knopoff [2], most earthquake catalogs exhibit a random character as their dominant statistical feature, the statistics of the small earthquakes being Poissonian [3].

Fluctuations of seismicity near the period of 1 year have been found, but in connection with the presence of artificial reservoirs. Several examples exist, as discussed by Gupta and Rastogi ([4], p. 114). Other examples are discussed, for example in Scholz [5] and in the review articles by Costain et al. [6] and Nicholson and Wesson [7]. The nature of seismicity at artificial reservoirs has been ascribed to the presence of fluids at depth and to the influence of varying pore pressure. An experiment to control the numbers of small earth-

* Tel.: +39-040-6762258; Fax: +39-040-575519; E-mail: berg@univ.trieste.it

0012-821X/00/$ – see front matter
PII: S0012-821X(00)00120-5

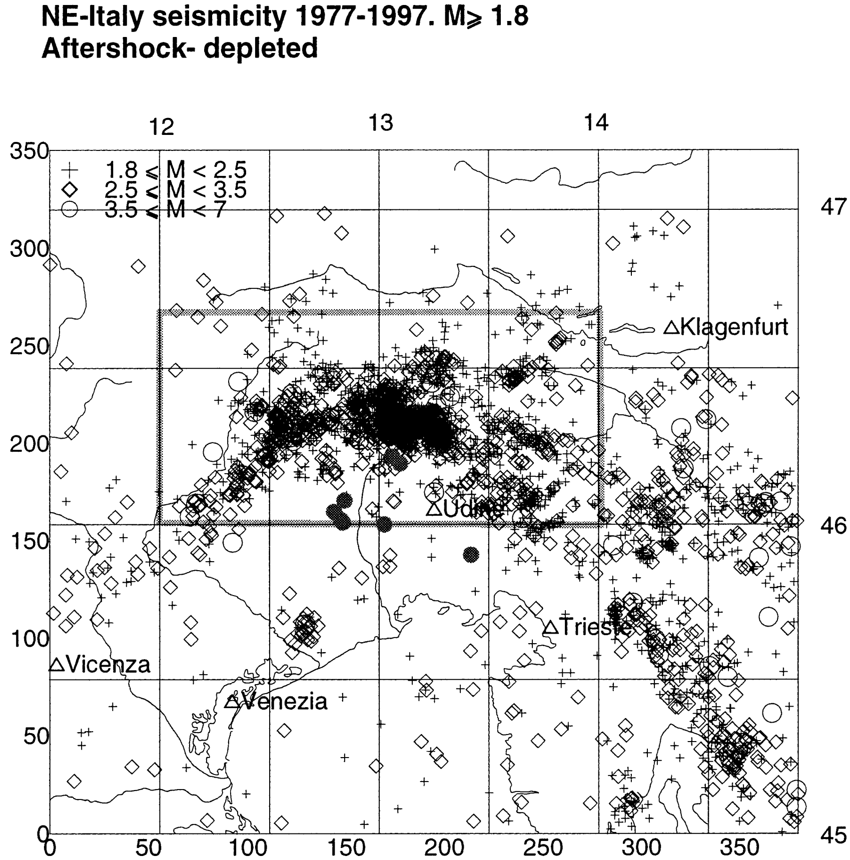

Fig. 1. Map of the studied area. The geographic distribution of seismicity is given as from the micro-seismicity catalogue of OGS for 1977–1997, $M \geq 1.8$. The gray dots show the positions of the wells. The gray rectangle limits the area over which seismicity is best defined and which was used for the spectral analysis.

quakes by manipulation of the fluid injection pressure was made at Rangely, CO, USA [8]. It was proven that the increase in pore pressure caused higher levels of seismicity.

At present, it is not proven that a variation on the time scale of a year or less is observed in natural seismicity. Some reported cases exist, which have put forward such a hypothesis. Kafri and Shapira [9] report on the correlation between earthquake occurrence, rainfall and water level of Lake Kinnereth (Israel). Roth et al. [10] discuss evidence for precipitation-induced seismic activity in the Swiss Alps. Muço [11] investigates the possibility of rainfall-induced earthquakes of $M \geq 4$ in the Balkan area.

Regarding the area of NE Italy, interpretation of strain-tilt measurements regarding the long [12,13] and short period observations [14] proposed the presence of quasi-periodicities at periods near 3–4 and 1–2 years in seismicity. The annual component in seismicity was also proposed by Westerhaus [15] in the study of strain-tilt observations in Turkey.

Geographically, the studied area is located in the northeastern part of Italy, bounded by Austria to the North and Slovenia to the East. The area is characterized by the interaction of two chains, the Dinarides and the Southern Alps. The system reflects the collision between the Adria microplate and the European plate. The seismicity is high and has led to destructive earthquakes also in this century. The seismotectonics and the structural framework are reported, for example, by Carulli et al. [16] and Slejko et al.

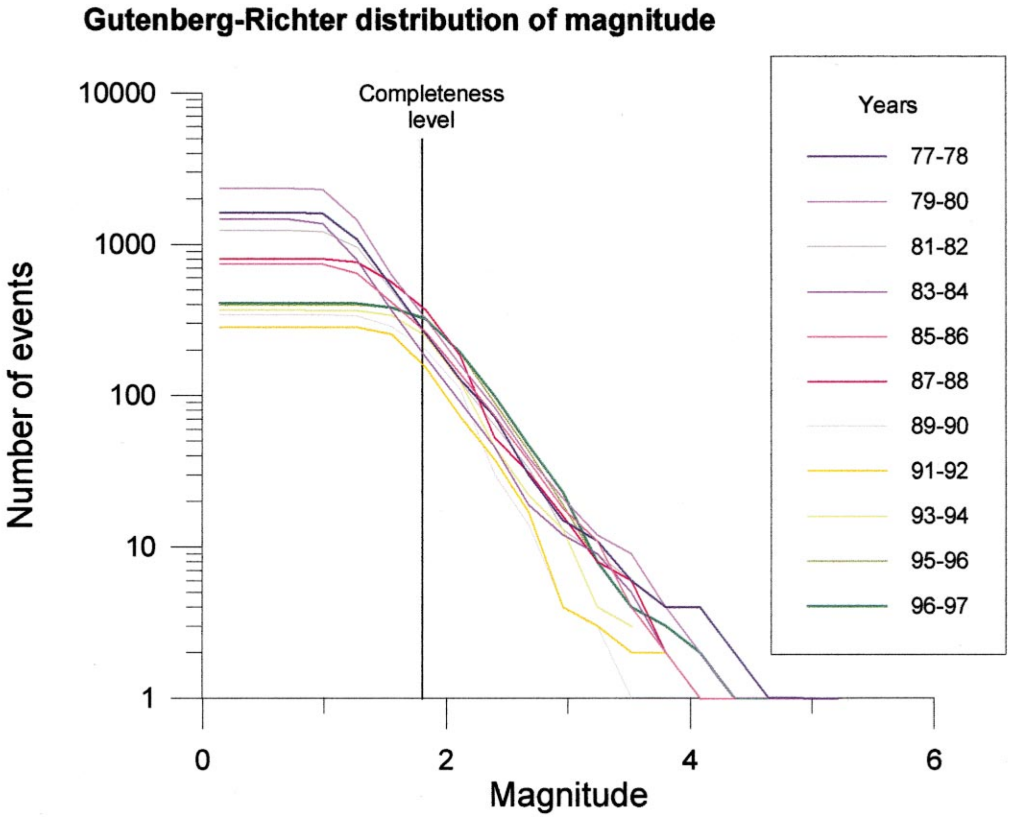

Fig. 2. Gutenberg–Richter curves of seismicity over two years for years 1977–1997. The completeness level can be estimated to be $M = 1.8$

([17] and references cited therein). The seismicity is shallower than 15 km, with a maximum value in the depth distribution at depths between 7 and 10 km.

2. Seismicity in time

The seismicity of Friuli (NE Italy) is recorded by the seismometric network of Friuli–Venezia Giulia (Istituto Nazionale Oceanografia e Geofisica Sperimentale, OGS), which started recording one year after the 1976 destructive earthquake ($M = 6.4$) of Friuli. Starting with only three stations during 1977, five more stations were added in 1978 and successively the network was increased by another seven stations until 1985. The acquisition system was analog from 1977 to 1987, in 1988 it was converted to a digital system. The introduction of a trigger system, which accepted only events recorded simultaneously on three stations, reduced the number of reported small events for the years 1988–1994. The digital acquisition system was upgraded in April 1994, with a trigger algorithm on each single station (Dr. G. Bressan, personal communication). For the years 1977–1987 the recorded events have been reprocessed and a revised catalogue has been published by Renner [18]. For the subsequent years, the catalogue released by the OGS-network has been published [19].

Fig. 1 shows a geographic map of the area with the main cities and the seismicity, for $M \geq 1.8$, over the years 1977–1997. Furthermore, the positions of the wells where the water table is measured are identified as gray dots. For the spectral analysis a smaller geographic window was defined, which comprises the area well covered by

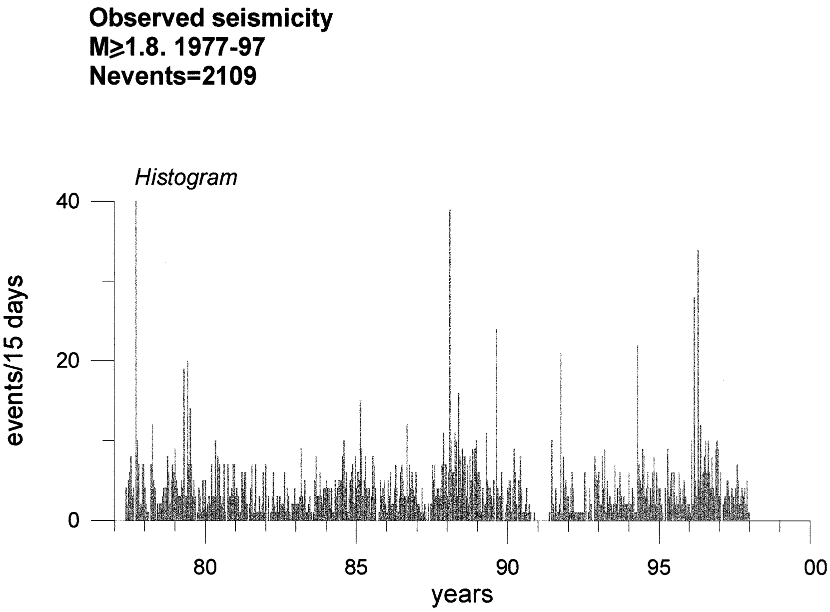

Fig. 3. Time evolution of seismicity. Full OGS catalogue, period 1977–1997, $M \geq 1.8$, noted as number of events in 15 days.

the micro-seismicity network. It is set to latitude (46–46.7°) and longitude (12–14°) and is shown as a gray rectangle in the figure.

The completeness level of the catalogue has been estimated to be $M = 1.8$. This was obtained from the deviation of the seismicity distribution from the Gutenberg–Richter law. The Gutenberg–Richter curves, calculated on sliding windows of two years, for the interval 1977–1997 are shown in Fig. 2. The vertical line shows the completeness level.

The histogram of seismicity (number of events) over the years 1977–1997 is shown in Fig. 3. The time base is equal to 1/24 year ($\sim$15 days). The magnitude has been limited to $M = 1.8$, which is the completeness level of the catalogue. The sharp peaks are due to aftershock sequences.

3. Aftershock depletion

To study the time evolution of the seismicity it is necessary to identify and remove aftershock sequences. If this is not done, the results are dominated and biased by main shocks which have a large number of aftershocks (see Fig. 3). One method is to use rectangular time–distance windows, which are dependent on the main shock magnitude (e.g. [3]). An improvement of this method is the use of a dynamic aftershock cluster-

Table 1
Number of clusters (n_{clu}) and of clustered events (n_{event}) identified by the clustering algorithm, for varying space (Q) and time parameters (P)

P	Q									
	2		5		10		15		25	
	n_{clu}	n_{event}	n_{clu}	n_{event}	n_{clu}	n_{event}	n_{clu}	n_{event}	n_{clu}	n_{event}
0.90	231	856	247	906	262	967	280	1027	299	1103
0.95	230	856	246	906	261	967	279	1027	298	1104
0.99	229	858	245	908	260	969	278	1030	296	1112

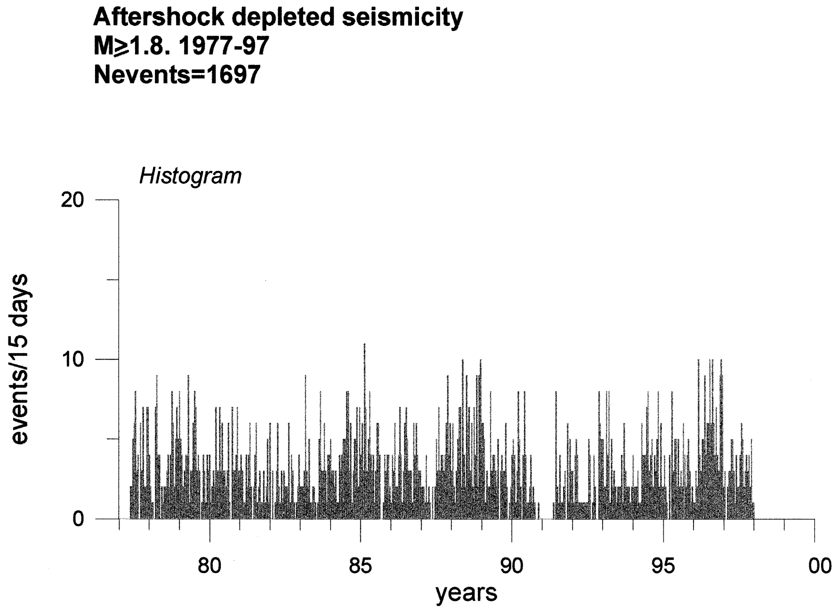

Fig. 4. Time evolution of seismicity. Depleted OGS catalogue, period 1977–1997, $M \geq 1.8$, noted as number of events in 15 days.

ing algorithm, which takes into account the fact that the extent in time and space of the aftershock sequences varies largely for different events [20]. The method of Reasenberg [20] uses a physical approach to the identification of aftershocks which states that each earthquake generates an alteration of the surrounding stress field that may trigger a further seismic event. Depending on a time parameter, this event is associated with the previous event and nucleates in its surroundings a modified stress field. The areal and time extent for which the event is liable to trigger a following event is termed the interaction zone of the event. The length scale for modeling the interaction zone is proportional to the source dimension, scaled by a parameter Q. The source dimension is modeled from existing empirical scaling relations as those found in [21]. The temporal extent of the interaction zone is determined with a probabilistic model based on Omori's law, which models the expected rate of aftershocks [20]. The parameter which governs the temporal extent is the confidence level P, at which it is assumed that the next event in the aftershock sequence is observed.

To assess the stability of the algorithm with respect to the space and time parameters, the algorithm is applied to the entire geographical area of the seismicity catalogue, over the interval 1977–1997, with a total number of events ($M \geq 1.8$) of 4257. The fault dimension is estimated by adopting the relation of Kanamori and Anderson [21] assuming a circular fault surface and the magnitude (M)–seismic moment (M_0) relation [22]:

$$\log M_0 = 9 + 1.5M \qquad (1)$$

the seismic moment being measured in Nm. Table 1 gives the number of clusters and the number of clustered events identified by the clustering algorithm, for varying space and time parameters Q and P. The test illustrated in Table 1 shows that the algorithm is almost insensitive to variation in P, whereas a greater influence is observed for the parameter Q. Increasing Q leads to an increase in the interaction zone of the events and consequently to an increase in the events declared as belonging to clustered events by the algorithm. The number of clusters decreases with increasing Q, as some clusters are merged together. We use the value of 10 for Q and set P equal to 0.95, which are the standard values proposed in the original paper [20].

The time evolution of the aftershock depleted catalogue is shown in Fig. 4, again as a histogram with 1/24 year sampling. The magnitude limit and the geographic window were chosen as above. The time series can now be analyzed without the bias due to the sharp peaks associated with the aftershock sequences.

To check for any depth dependence the analysis will be made for different depth ranges of seismicity. In order to have equal statistical significance, the depth windows are chosen so as to include the same number of events. The depth distributions of the events of the full and depleted catalogues are shown in Fig. 5a,b, respectively. The geographic window and magnitude limit is set as above. The maximum of the depth distribution lies between 7 and 14 km. The normalized integral of the depth distribution (heavy curve) is a function of depth and is equal to the percentage of seismic events which lie between the surface and the depth considered. We chose three overlapping depth classes, each of which contains 50% of the seismic events and is separated by 25% marks of the normalized depth integral. The three depth classes and the respective percentage points are given in Table 2. A fourth class is defined which covers the entire depth range of the seismicity. The only non-overlapping depth windows are those of the first and third class.

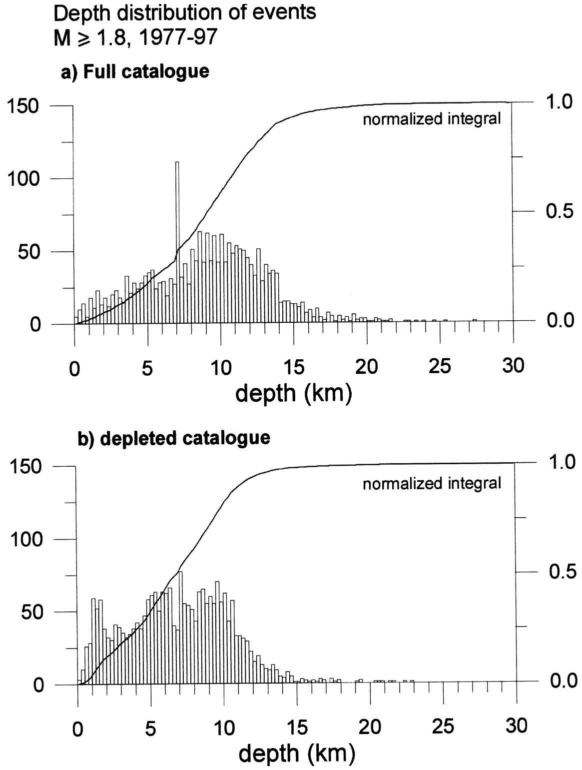

Fig. 5. Depth distribution of seismicity in Friuli (depleted OGS catalogue), period 1977–1997, $M \geq 1.8$, depth interval = 0.25 km. Superposed (heavy line) is the normalized depth integral. Left axis: number of events in depth interval; right axis: normalized depth integral.

4. Spectral analysis

For the purpose of analysis of the time evolution, the seismicity is treated as a point process. Given a time resolution, the sequence attains a value 1 or 0, depending on whether in the respective time bin an event has or has not occurred. The analysis is carried out for the time window 1.1.1977–31.12.1997. The amplitude spectrum is calculated from the Fourier transform of the sequence. Band averaging is applied, so as to obtain

Table 2
Normalized integral percentage values of the depth distribution of the seismicity for four depth classes

Depth class	Upper depth	Lower depth	Percentage value		Number of eventsevents	
	(km)	(km)	upper depth	lower depth	full catalogue	depleted catalogue
1	0	9.3	0	50	1089	846
2	6.3	11.9	25	75	1089	845
3	9.3	30	50	100	1032	862
4	0	30	0	100	2109	1697

Depleted OGS catalogue, period 1977–1997, $M \geq 1.8$. The numbers of events which fall into each depth class for both the full catalogue and the depleted catalogue are given.

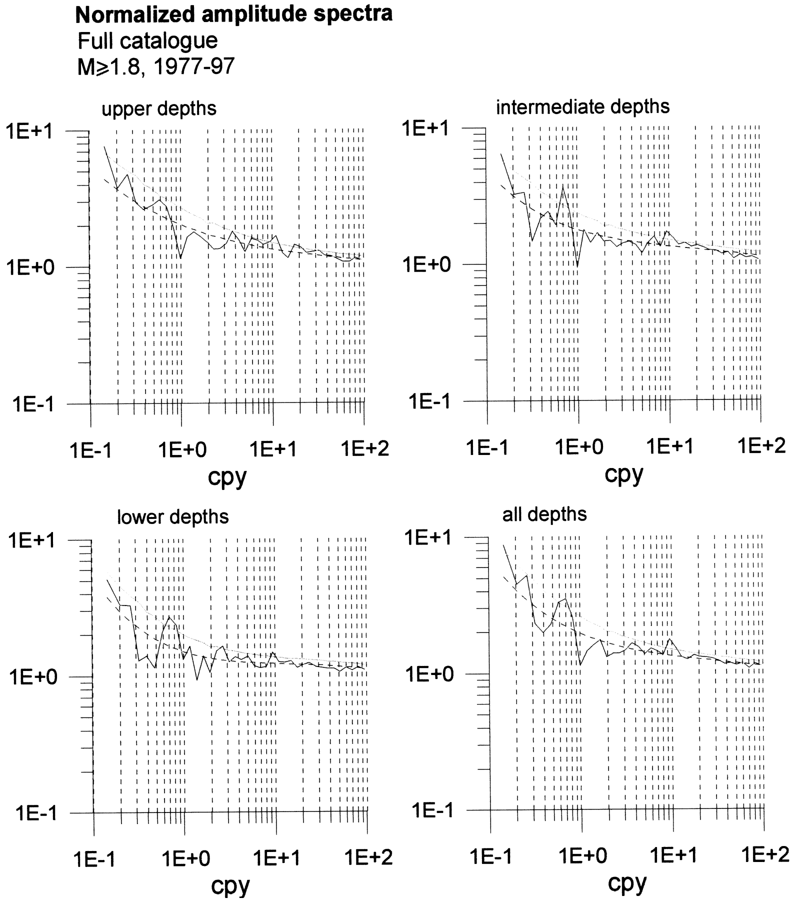

Fig. 6. Amplitude spectra of the seismicity for four overlapping depth classes. Frequency in cycle per years. The spectral amplitudes are normalized to the values of a pure Poisson distributed seismicity. Also shown are the reference level and the 95% significance level. Full seismic catalogue. The depth classes are as given in Table 2.

15 spectral values per decade. We normalize the spectrum by the value expected for a purely Poisson distributed seismicity of the same seismicity rate k. Given a sequence N time bins long, the expected spectral power is uniform with value k/N, except at the origin where it attains the value k^2 ([23], p. 245). The average seismicity rate k is obtained from the total number of events in a given magnitude and depth class, divided by the total elapsed time.

The significance of a spectral peak is ascertained if it is significantly higher than the mean spectrum in that frequency band. The mean spectral amplitude is calculated from a polynomial approximation of the entire spectrum, where the polynomial is allowed to have an order up to 4 degrees. The significance limit of the observed spectral values of the real catalogue is estimated from the χ^2 distribution (e.g. [24,25]) at a 95% confidence level. That is, at each frequency the upper limit of the spectral value is calculated, which could be obtained at the 95% confidence limit, given the number of degrees of freedom used.

The amplitude spectra of the seismicity pertaining to the four depth classes are graphed in Figs. 6 and 7 for the full and depleted catalogues, respectively. The continuous line is the observed amplitude spectrum, the dashed line is the polynomial reference spectrum and the gray line is the

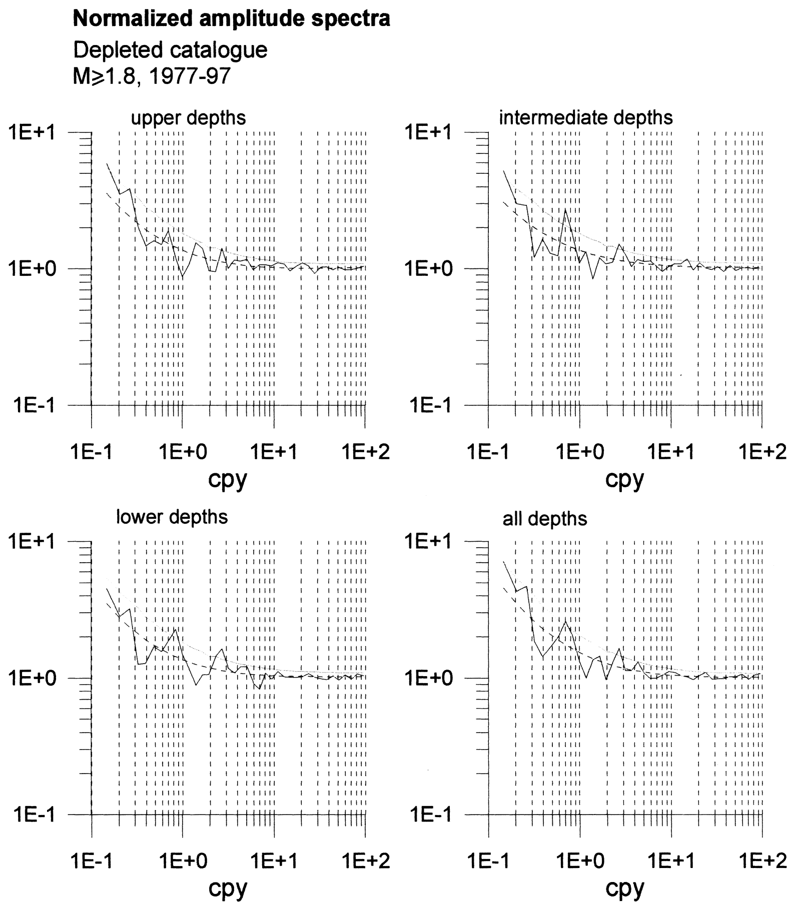

Fig. 7. Amplitude spectra of the seismicity for four overlapping depth classes. Same as Fig. 6, except for depleted seismic data.

95% confidence level of the spectrum. The spectra decay from lower to higher frequencies, stabilizing at a near to constant level for frequencies greater than 10–100 cpy. A significant spectral energy peak, common to the full and depleted catalogues, is found at about 0.7 cpy. The peak is less pronounced for the most shallow depth class and is largest for the intermediate depth class. The maximum of the depth distribution falls into this intermediate depth class. At higher frequencies some spectral values emerge above the 95% significance mark, but are generally not consistent over all depth windows. A significant but weak spectral energy appears to be consistent in all depth classes at about 10 cpy in the spectrum of the full catalogue, but it vanishes after aftershock depletion.

To investigate the dependence of the spectral component at 0.7 cpy on the magnitude threshold level, the spectral analysis is repeated for different thresholds. The minimum magnitude is raised by steps of 0.2 from $M = 1.8$ to $M = 4.0$. Again the events are selected according to four depth classes (superficial, intermediate, deep, all) and the depleted catalogue was used. The results are shown in Fig. 8, where the spectral amplitude at 0.7 cpy, the spectral reference level and the 95% significance level are displayed for different minimum magnitudes. The number of events ranges from 1697 for the events with $M \geq 1.8$ to 12 events with magnitudes $M \geq 4.0$, for depth class four. The number of events decreases to about half this value for the other depth classes. It is seen that the spectral component is significantly differ-

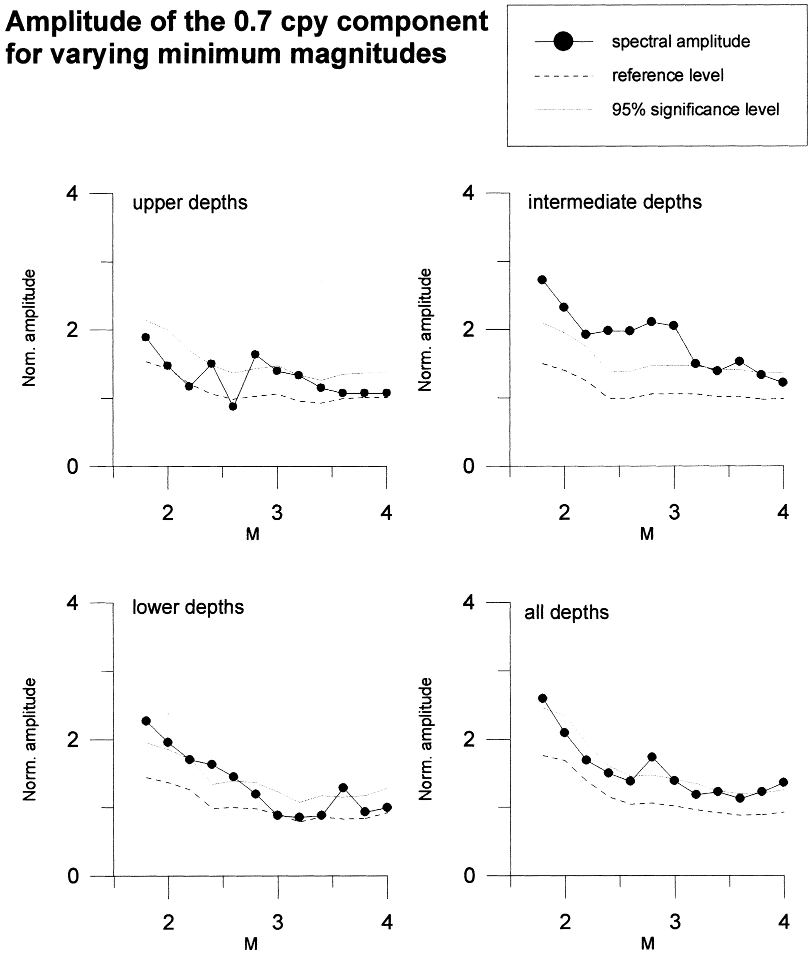

Fig. 8. Spectral amplitude of seismicity at the frequency of 0.7 cpy in dependence on the threshold magnitude. Also shown are the reference level and the 95% significance level. The spectral values are normalized to the values of a pure Poisson distributed seismicity. Depleted catalogue. Depth classes as defined in Table 2.

ent than the reference level at depth classes 2 and 3 for threshold magnitudes between 1.8 and 3 or 2.6, respectively. The spectral amplitude for depth classes 1 and 4 is rather normal, except for magnitude threshold 2.8.

5. Discussion and conclusions

The seismicity of NE Italy has been studied with intent to test whether non-random features are reflected in the data. The catalogue of the OGS micro-seismicity network was used, which covers the years 1977–1997, at a completeness level of $M = 1.8$.

In order to avoid the bias due to the presence of aftershock sequences, an aftershock depleted catalogue was built and the analysis carried out for both the full and depleted catalogues.

The spectral analysis reveals the presence of a significant fluctuation in the number of events, with a mean return period of 1.4 years, equivalent to 0.7 cpy. This is a considerably lower frequency than the yearly period which is characteristic of seasonal atmospheric agents as temperature and pressure.

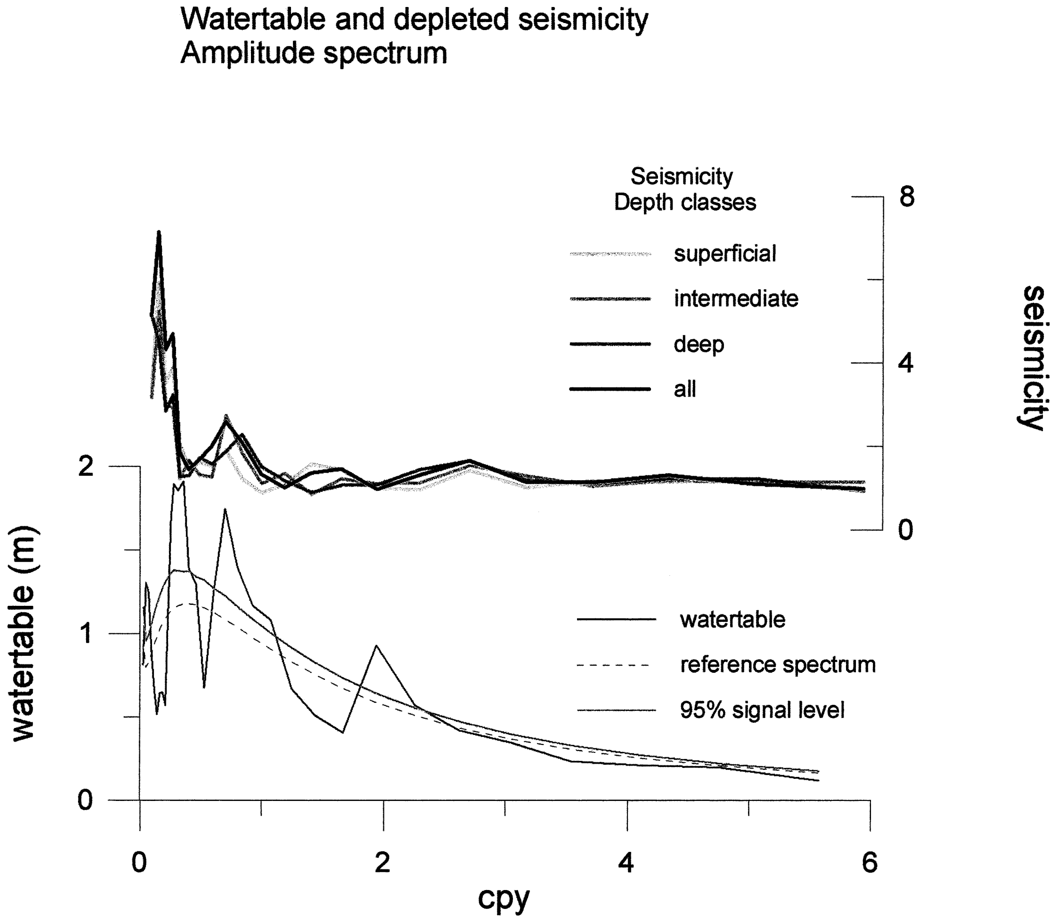

Fig. 9. Amplitude spectra of average water table and seismicity. The spectral values of seismicity are normalized to the value expected for a Poisson distributed seismicity.

A similar frequency in the spectral content is in fact observable in the time variation of the water table. We have inspected eight wells in NE Italy, with continuous data records covering the time interval from 1977 to 1997. The observations, furnished by the Regione Friuli–Venezia Giulia, have a sampling of 3 or 6 days. These data were linearly interpolated to 1 day intervals and the amplitude spectra were calculated for each well. From the eight spectra an average spectrum was obtained, which is taken as representative of the average time variation of the water table in the region. As for the seismic spectral analysis, the frequency sampling was set to 15 samples per decade. The mean spectrum is plotted in Fig. 9, where the spectrum can be seen to include three principal constituents, namely at frequencies 0.33, 0.7 and 2 cpy. The spectral peaks are significant, as they lie above the 95% confidence level of the reference spectrum. Again, the reference spectrum was obtained by a polynomial approximation of the observed spectrum. For comparison the seismicity amplitude spectra are redrawn in Fig. 9. No conclusions can be drawn regarding the existence of the 0.33 cpy frequency here, as low frequencies are not well resolved. Apart from the well resolvable spectral component of 0.7 cpy, the component of 2 cpy is not present in seismicity. At this stage we can put forward the working hypothesis that the spectral component of 0.7 cpy in the micro-seismicity could be related to variations in the water table or could be due to a common cause, as for example the melting of the snow cover in the mountains North of the seismic zone. It remains unclear, however, why then the spectral component of 2 cpy, evident in the water table variation, is not observed in the seismicity.

As shown by Rydelek and Sacks [26], a periodicity in a seismic catalogue is liable to be observed, if the noise level changes periodically. This was the explanation for the fact that catalogues of small threshold magnitudes of different areas may contain a diurnal periodicity, due to lower seismic noise at night. Similarly this may also happen at lower frequencies, as for instance in our case. This would mean that the observation of the periodicity does not reflect a physical variation of the level of seismicity, but rather a variation in the noise level of the recording system. So far, no explanation or cause has been found for the fact that the noise level varies with a period of 1.4 years.

If the spectral component is due to a real fluctuation in seismicity, it is probable that it would be found also in the micro-seismicity recorded in other areas. It should be investigated in the future, whether other micro-seismicity catalogues contain a near to yearly fluctuation in the rate of small events. It could then be studied what these areas have in common with the Friuli area, regarding the geology, fault mechanisms and perhaps also the hydrological characteristics. Furthermore, the different seismic areas will be mapped according to whether the micro-seismicity rate is purely random, or has a deviation on a near to yearly periodicity. One problem is that such analysis requires catalogues which cover a long period, to obtain reliable spectral estimates at these low periodicities.

Acknowledgements

The OGS is thanked for making the seismicity catalogue available. The Regione Friuli–Venezia Giulia is thanked for the availability of the water table records. Dr. Paul Reasenberg is thanked for use of the aftershock depletion algorithm. Professor Maria Zadro is thanked for constructive advice. Professor Ad Aertsen, Professor Peter Suhadolc and Dr. Dario Slejko are thanked for discussions. Professor Gerhard Jentzsch is thanked for his review of the paper. The work was partly financed by EC Research Grant IC15 CT96-0205, MURST 40% and CNR 98.00159/97.00121.***[EB]***

References

[1] S. Kilston, L. Knopoff, Lunar–solar periodicities of large earthquakes in southern California, Nature 304 (1983) 21–25.
[2] Y. Kagan, L. Knopoff, Statistical search for non-random features of the seismicity of strong earthquakes, Phys. Earth Planet. Interact. 12 (1976) 291–318.
[3] J.K. Gardner, L. Knopoff, Is the sequence of earthquakes in Southern California, with aftershocks removed, Poissonian?, Bull. Seismol. Soc. Am. 64 (1974) 1363–1367.
[4] H.K. Gupta, B.K. Rastogi, Dams and Earthquakes, Elsevier, Amsterdam, 1976.
[5] C.H. Scholz, The Mechanics of Earthquake Faulting, Cambridge University Press, Cambridge, 1990.
[6] J.K. Costain, G.A. Bollinger, J.A. Speer, Hydroseismicity: a hypothesis for the role of water in the generation of intraplate seismicity, Seism. Res. Lett. 58 (1987) 41–64.
[7] C. Nicholson, R.L. Wesson, Triggered earthquakes and deep well activities, Pure Appl. Geophys. 139 (1992) 561–578.
[8] C.B. Raleigh, J.H. Healy, J.D. Bredehoeft, An experiment in earthquake control at Rangely, Colorado, Science 191 (1976) 1230–1237.
[9] U. Kafri, A. Shapira, A correlation between earthquake occurrence, rainfall and waterlevel in Lake Kinnereth, Israel, Phys. Earth Planet. Interact. 62 (1990) 277–283.
[10] Ph. Roth, N. Pavoni, N. Deichmann, Seismotectonics of the eastern Swiss Alps and evidence for precipitation-induced variation in seismic activity, Tectonophysics 207 (1992) 183–197.
[11] B. Muço, Statistical investigation on possible seasonality of seismic activity and rainfall-induced earthquakes in Balkan area, Phys. Earth Planet. Interact. 114 (1999) 119–127.
[12] G. Rossi, Fractal analysis as a tool to evidence seismic cycle phases, in: J. Kruhl (Ed.), On Fractals and Dynamic Systems in Geoscience, Springer Verlag, Berlin, 1994, pp. 169–176.
[13] G. Rossi, M. Zadro, Long-term crustal deformations in NE Italy revealed by tilt-strain gauges, Phys. Earth Planet. Interact. 97 (1996) 55–70.
[14] C. Braitenberg, M. Zadro, Strain, seismicity and rain, in: Proceedings of the XXIV General Assembly of the European Seismological Commission, 19–24 September 1994, Athens, 1996, pp. 1216–1224.
[15] M. Westerhaus, Tidal tilt modification along an active

fault, in: H. Wilhelm, W. Zürn, H.-G. Wenzel (Eds.), Tidal Phenomena, 1998, pp. 311–339.
[16] G.B. Carulli, R. Nicolich, A.. Rebez, D. Slejko, Seismotectonics of the northwestern Dinarides, Tectonophysics 179 (1990) 11–25.
[17] D. Slejko et al., Modello sismotettonico dell'Italia nord-orientale. C.N.R. G.N.D.T. Rendiconto 1, Ricci, Trieste, 1987, pp. 1–82.
[18] G. Renner, The revision of the northeastern Italy seismometric network catalogue, Boll. Geof. Teor. Appl. XXXVII (1995) 229–505.
[19] Anonymous, Bollettino Rete Sismometrica Friuli-Venezia Giulia, Osservatorio Geofisico Sperimentale, Trieste, 1999.
[20] P. Reasenberg, Second-order moment of Central California seismicity, 1969–1982, J. Geophys. Res. 90 (1985) 5479–5495.
[21] H. Kanamori, D.L. Anderson, Theoretical basis of some empirical relations in seismology, Bull. Seism. Soc. Am. 65 (1975) 1073–1095.
[22] T.C. Hanks, H. Kanamori, A moment magnitude scale, J. Geophys. Res. 84 (1979) 2348–2350.
[23] Y.W. Lee, Statistical Theory of Communication, J. Wiley and Sons, New York, 1960, 509 pp.
[24] R.B. Blackman, J.W. Tukey, The Measurement of Power Spectra, Dover, New York, 1958, 190 pp.
[25] J. Taubenheim, Statistische Auswertung geophysikalischer und meteorologischer Daten, Akademische Verlagsgesellschaft Geest und Portig, Leipzig, 1969, 386 pp.
[26] P.A. Rydelek, I.S. Sacks, Testing the completeness of earthquake catalogues and the hypothesis of self-similarity, Nature 337 (1989) 251–253.